

Influence of Silicon Carbide Filler on Mechanical and Dielectric Properties of Glass Fabric Reinforced Epoxy Composites

B. Suresha,¹ G. Chandramohan,² N. M. Renukappa,³ Siddaramaiah⁴

¹Department of Mechanical Engineering, National Institute of Engineering, Mysore 570008, India

²Department of Mechanical Engineering, PSG College of Technology, Coimbatore-641004, India

³Department of Electronics and Communication Engineering, Sri Jayachamarajendra College of Engineering, Mysore 570006, India

⁴Department of Polymer Science and Technology, Sri Jayachamarajendra College of Engineering, Mysore 570006, India

Received 29 May 2006; accepted 24 June 2008

DOI 10.1002/app.29116

Published online 13 October 2008 in Wiley InterScience (www.interscience.wiley.com).

ABSTRACT: Fiber-reinforced polymeric composites (FRPCs) have emerged as an important material for automotive, aerospace, and other engineering applications because of their light weight, design flexibility, ease of manufacturing, and improved mechanical performance. In this study, glass-epoxy (G-E) and silicon carbide filled glass-epoxy (SiC-G-E) composite systems have been fabricated using hand lay-up technique. The mechanical properties such as tensile strength, tensile modulus, elongation at break, flexural strength, and hardness have been investigated in accordance with ASTM standards. From the experimental investigations, it has been found that the tensile strength, flexural strength, and hardness of the glass reinforced epoxy composite increased with the inclusion of SiC filler. The results of the SiC (5 wt %)-G-E com-

posite showed higher mechanical properties compared to G-E system. The dielectric properties such as dielectric constant (permittivity), tan delta, dielectric loss, and AC conductivity of these composites have been evaluated. A drastic reduction in dielectric constant after incorporation of conducting SiC filler into epoxy composite has been observed. Scanning electron microscopy (SEM) photomicrographs of the fractured samples revealed various aspects of the fractured surfaces. The failure modes of the tensile fractured surfaces have also been reported. © 2008 Wiley Periodicals, Inc. *J Appl Polym Sci* 111: 685–691, 2009

Key words: glass fabric reinforced epoxy composite; SiC filler; mechanical properties; electrical properties; failure mechanisms

INTRODUCTION

Fiber reinforced polymeric composites (FRPCs) are advanced engineering material systems for automotive, aerospace, and other engineering applications because of their high strength and modulus coupled with light weight, design and fabrication flexibility, and improved mechanical performance. The most common fiber reinforcements for polymer composites are glass, carbon (graphite), and aramid (Kevlar 49) fibers. These composites, not only retain high strength, high stiffness, and thermal resistance, but also show enhanced impact strength, fatigue resistance, and dimensional stability.^{1,2} One of the most commonly used polymeric composite is glass fiber reinforced polymeric (GFRP) composite material. E-glass fibers are created using a calcium alumina borosilicate formulation that produces beneficial me-

chanical properties at very reasonable cost as compared to carbon and Kevlar fibers. The purpose of the matrix in a fiber reinforced polymer (FRP) composite material is to bind the fibers together, to transfer load to the fibers, and to protect them from environmental conditions and handling damages. The most common matrix materials are epoxy, polyester, vinyl ester, etc. Among these, polyester and epoxies possess excellent mechanical properties, and good chemical and corrosion resistance.³ Also, these resins in molded or cast form have excellent dimensional stability and low shrinkage. Further, these materials offer the advantage of easy processability by merely adding a curing agent with or without the application of heat.

Automotive and aircraft components⁴ fabricated with FRPCs have stringent requirements and are required to withstand mechanical damages during service. Kim et al.⁵ reported that the fiber damage could occur during the fabrication process, storage, service, transport, and maintenance. Polymeric composite materials are susceptible to mechanical damages and interlayer delamination when subjected to

Correspondence to: Dr. B. Suresha (sureshab2004@yahoo.co.in).

effects of tension, compression and flexure. Varada Rajulu et al.⁶ investigated the tensile properties of glass rovings reinforced epoxy toughened with hydroxyl-terminated polyester composites and reported that the tensile strength increased with increase in fiber content. Fracture performance of FRPCs is mostly dominated by the following failure mechanisms: (a) matrix plastic deformation and matrix fracture; (b) related to fiber/matrix interface, matrix/fiber debonding and fiber pull-out; and (c) fiber fracture.^{7,8} The service temperature, duration, and magnitude of stress also decide the failure mechanism of composite materials. The nature of the reinforcing fiber also affects the strength, durability, thermal conductivity, creep resistance, and also the failure of the polymeric matrix composite.⁹ The literature reveals that the type of fiber and its orientation, matrix and filler influence the strength, stiffness, and other mechanical properties of the composites.⁶⁻¹⁵

Most of the above findings are based on either randomly oriented or unidirectionally oriented fiber composites. Woven fabric reinforced composites are gaining popularity because of their balanced properties in the fabric plane as well as their ease of handling during fabrication.¹⁶ Mody et al.¹⁷ have shown that the simultaneous existence of parallel and perpendicular oriented carbon fibers in a woven configuration leads to a synergistic effect on the enhancement of the wear resistance of the composite. Furthermore, it has been reported that thermoset resins reinforced with fillers and fibers possess very good mechanical and tribological properties.¹⁸ Inclusion of particulate fillers to glass reinforced polymer composites results in a new family of hybrid laminates with an ability to impede and slow down the elongation caused by tensile loading. Most studies on filler action in the case of polymer composites sliding against metallic counter faces have focused on the reduction of wear rate and coefficient of friction. In addition to the higher mechanical strength obtained due to the addition of fillers in polymeric composites, there is direct cost reduction because of the less consumption of resin material. The critical and final selection of filler primarily depends upon the requirements of the end product, the interface compatibility, and the dimension/shape of particles. Incorporation of a higher percentage of particulate filler in FRPC leads to agglomeration while an optimum percentage of filler improves the mechanical properties significantly.

The use of composite materials in engineering as dielectric is becoming increasingly important. Therefore studies on the dielectric properties of FRPCs are very important. Many researchers have studied the dielectric properties of conducting filler and fiber filled FRPCs.¹⁹⁻²² Boonstra and Dannenberg¹⁹ have investigated the variation of conductivity of rubber-

carbon black (CB) vulcanizates with various parameters such as concentration of CB, processing parameters, deformation, temperature, grain size, and surface area of CB. They have given a qualitative explanation for these experimental results. They suggested that there exists continuous chains of conducting particles in the matrix and that these chains are responsible for the flow of current. Read and Stow²⁰ report the dependence of current on voltage and the dependence of resistance on temperature and frequency for a rubber-CB system. The order of magnitude of resistivity of the samples they have used is 109 Ω cm. The V-I characteristics of the samples appear to exhibit either a square law characteristics or an exponential characteristics. Garcia and Bahder²¹ have investigated the effect of temperature on resistivity of polyethylene loaded with 33 and 35% by weight of CB. They have found that conductivity decreases with temperature. Amin and Hassan²² have studied the variation of resistivity with temperature for styrene-butadiene rubber (SBR) charged with 50 parts by weight of CB. They report that conductivity decreases in the low temperature region and beyond a point of minimum conductivity it increases with temperature. They have found that the temperature at which the minimum conductivity occurs decreases when the above composition is blended with polyvinyl chloride (PVC). Evaluation of dielectric properties of the composites may help in tailoring the polymer composites for various applications.

An understanding of mechanical and dielectric properties of polymeric composites is necessary for industrial applications. Hence, in the present work, E-glass woven fabric reinforced epoxy with and without SiC particulate filler have been investigated and characterized for mechanical as well as dielectric properties.

EXPERIMENTAL

Materials

Woven E-glass fabric (Density 2.54 g/cm³ and modulus 72.4 GPa) having fibers of diameter 8–12 μ m were used as a reinforcing material in epoxy composites. The matrix was a medium viscosity epoxy resin (LAPOX L-12) and a room temperature hardener with a tetra amine functional group (K-6) supplied by ATUL India Ltd, Gujarat, India was used. SiC of particle size in the range 25–40 μ m, procured from the local market was used as the filler material.

Fabrication of composite laminate and test specimens

E-glass woven roving fabric was placed on a teflon sheet over which the epoxy resin mixed with the

TABLE I
Typical Formulation of Composites with Sample Code

Sample code	Matrix	wt %	Reinforcement	wt %	wt % of silicon carbide filler
G-E	Epoxy	50 ± 2	E-glass fabric	50 ± 2	0.0
SiC-G-E	Epoxy	45 ± 2	E-glass fabric	50 ± 2	5.0

hardener in the ratio 100:12 by weight was smeared. Dry hand lay up technique was employed to fabricate the composites. The stacking procedure consisted of placing the fabric one above the other with the resin mix well spread between the fabrics. The process was repeated till all the eight layers were used up in the stacking sequence and a 3-mm laminate was obtained. A porous teflon film was again used on top to cover the stack. To ensure uniform thickness of the sample, a 3-mm spacer was used. The mold plates were coated with release agent to aid the ease of separation on curing. The whole assembly was kept in a hydraulic press at a pressure of 0.5 MPa and allowed to cure for a day at room temperature. The slabs so prepared measured 250 mm × 250 mm × 3 mm by size. To prepare silicon carbide particulate filled epoxy composite; besides the resin hardener mixture additional 5% filler particles by weight were included to form the resin mix. The detailed compositions of the composites (including wt % of the constituents) processed are shown in Table I. The test specimens were prepared from a diamond tipped cutter as per ASTM standards.

Techniques

The capacitance and tan delta values of composite specimens were measured as per ASTM D 149 standard using precision LCR meter model 4285A and model 4192A Hewlett-Packard, USA, in the frequency range 100 Hz–30 MHz. The samples employed for electrical properties measurements were circular discs, which were sandwiched between brass electrodes (11.3 cm²). The dielectric constant (ϵ) of the composites was calculated by using the equation;

$$\epsilon = \frac{C_d}{\epsilon_0 \times A} \quad (1)$$

where, C (p_f) is the capacitance, d (cm) is the thickness of the sample, ϵ_0 is absolute permeability, a constant equal to 8.854×10^{-12} , and A (cm²) is the area. The imaginary part of the dielectric loss, ϵ' was calculated using the relation;

$$\epsilon' = \epsilon \tan \delta \quad (2)$$

and the AC conductivity (σ) was calculated by using the equation;

$$\sigma = \omega \epsilon' = 2\pi f \epsilon' \quad (3)$$

where, f (Hz) is the frequency and ω (rad/s) is angular frequency.

The mechanical properties such as tensile strength, tensile modulus, elongation at break, and flexure properties, were investigated using Universal tensile testing machine (JJ Lloyd, London, United Kingdom, capacity 1–20 kN) in accordance with ASTM D 638 and ASTM D 790 methods, respectively. The tensile and flexural tests were performed at a crosshead speed of 5 mm/min and 2 mm/min, respectively. Five samples were tested for each composition of the composites. Hardness of unfilled and SiC filled thermoset composites were measured using the Rockwell hardness tester (Rockwell C, make; Newage testing instruments, Inc., Southampton, USA)

Scanning electron microscopy (SEM) is the most widely used imaging technique for the study of FRPCs. A scanning electron microscope was used to analyze the fracture surface of the composites. A section of the tensile fractured surface samples were mounted on aluminum stub using conductive (silver) paint and were sputter coated with gold prior to fractographic examination. The SEM (Leica, XL30 SEM with an Oxford ISIS310 EDX, Cambridge instruments, Cambridge England) micrographs were obtained under conventional secondary electron imaging conditions with an acceleration voltage of 25 kV.

RESULTS AND DISCUSSION

Electrical properties

The effect of SiC filler on the electric properties such as dielectric constant (permittivity), tan delta, dielectric loss, and AC conductivity of the composites have been studied. Variation of dielectric constant as a function of log frequency for G-E and SiC-G-E composites is shown in Figure 1. The figure indicates a drastic reduction in dielectric constant after incorporation of SiC as filler into G-E composites. This is due to; (i) increase in conducting phase due to the incorporation of SiC in which SiC fillers

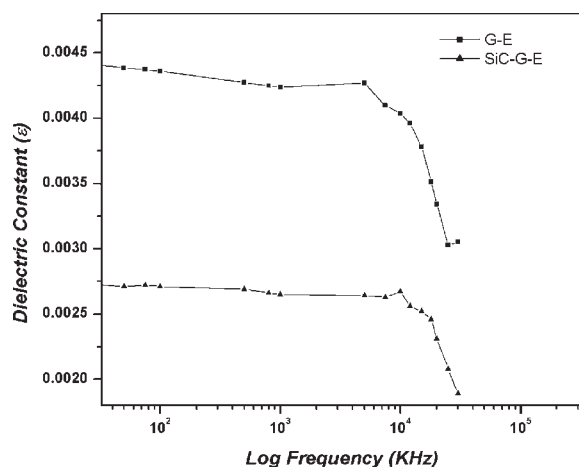


Figure 1 Effect of dielectric constant versus frequency of G-E and SiC-G-E composites.

interact imparting conductivity and (ii) reduction in void content of glass fiber reinforced composites, as the voids are now filled with SiC fillers. These two factors reduce the dielectric constant of composites as expected. The permittivity (dielectric constant) of insulators relative to free space is always greater than unity. In the case of semiconductors, there are few free electrons, which partly shield the bound charges from the electric field, and hence their relative permittivities are smaller than that of insulators. In case of conductors, the number of free electrons is so large that the bound charges are practically shielded from the electric field, and thus no polarization occurs. The variation of dielectric constant of FRPC is directly influenced by incorporation of SiC filler.

The plot of tan delta versus log frequency is shown in Figure 2 for G-E and SiC-G-E composites. From the figure it may be noticed that the tan delta values of all the composite compositions are identical up to 10^3 kHz of frequency. A sharp change in tan delta values for both composites was noticed around 10^4 kHz frequencies. There is no systematic variation in tan delta values beyond 10^4 kHz. The drastic change in tan delta values above 10^3 kHz of frequency is due to phase transition, which occurred because of change in temperature. At higher frequencies, $\tan \delta$ significantly increases, because of orientation polarization resulting from chain motion of polymer.

The variation of dielectric loss as a function of log frequency for G-E and SiC-G-E composites is shown in Figure 3. From the figure it was observed that there was no significant influence of frequency on dielectric loss of all the composites up to 10^3 kHz frequencies. Above 10^3 kHz a steep increase in dielectric loss is observed for both the composite specimens. However, the loss factor is on the higher

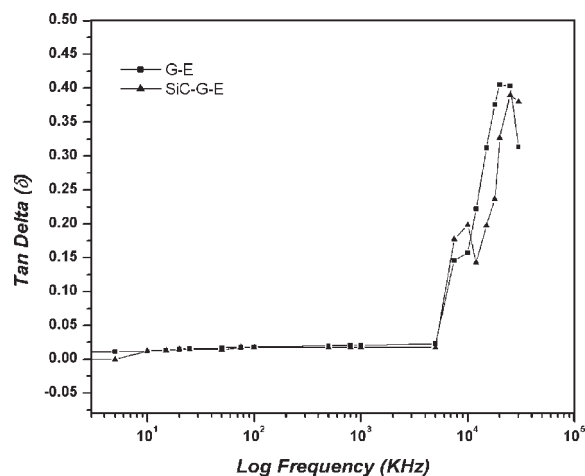


Figure 2 Variation of tan delta as a function of frequency of G-E and SiC-G-E composites.

side for unfilled G-E composite specimen. A peak is found for both the curves at around a frequency of $10^{4.1}$ kHz due to strong relaxation. These loss factor peaks may be attributed because of dielectric relaxation involving interfacial polarization.

The plot of AC conductivity as a function of log frequency is shown in Figure 4. No variation in conductance values is observed for the frequency range of 10^1 kHz to 10^2 kHz. However, above 10^2 kHz frequency a drastic increase in conductivity is observed. A steep increase in conductance values from 10^{-6} S/m to 10^{-1} S/m in the frequency range of 10^2 kHz to 5×10^5 kHz is observed for SiC-filled G-E composite. This can be attributed to the increase in orientation of molecules with the applied electric field. The pattern of variation in conductance is identical for all formulations and there is no systematic variation in AC conductivity. The trend of variation in AC conductivity is similar to that of tan delta

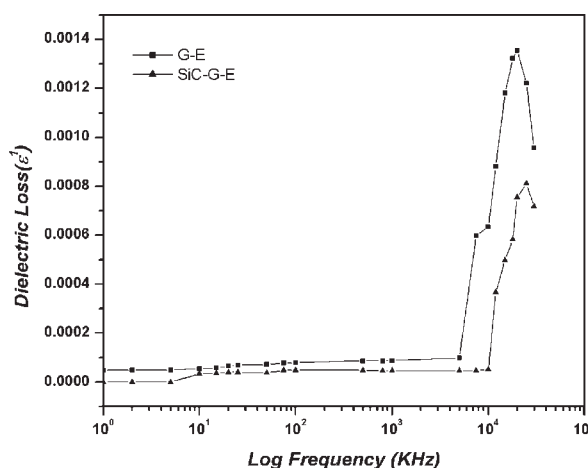


Figure 3 Plot of dielectric loss versus frequency of G-E and SiC-G-E composites.

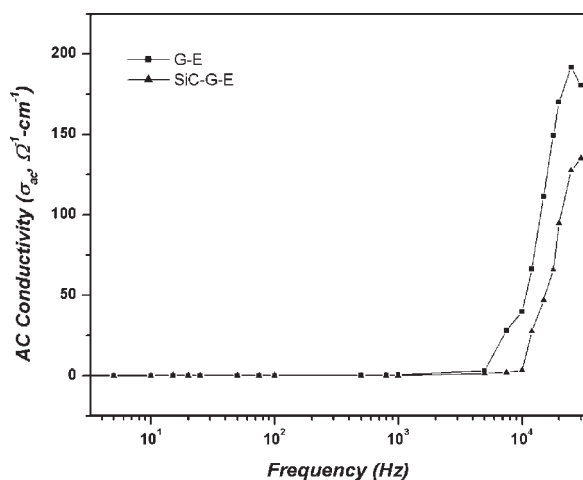


Figure 4 Plot of AC conductivity as a function of frequency of G-E and SiC-G-E composites.

and dielectric loss. AC conductivity of the matrix at the lowest loading of the filler is affected by three parameters i.e., the intrinsic conductivity of the filler, the shape of the filler and the surface tension of the matrix and the filler. It is expected that fibrous fillers yield a percolation threshold at lower loadings as compared with irregularly shaped particles, since the former will afford many more inter particle contacts. Here the particles are not fibrous but are hard SiC particles. Therefore, with increase in frequency the AC conductivity is decreased.

Mechanical properties

The stress versus strain curves for G-E and SiC-G-E composites are shown in Figure 5. The mechanical properties depend to a greater extent on the reinforcement/filler and to a lesser extent on the matrix material and the interface/interaction between them. From Figure 5, it is clear that the stress-strain curve of SiC-filled G-E shows higher tensile strength. The measured tensile behavior and surface hardness test results of the G-E and SiC-G-E composites are recorded in Table II. Silicon carbide is composed of tetrahedral crystals of carbon and silicon atoms with strong bonds in the crystal lattice. This produces a very hard and strong material that has the ability to provide reinforcement. A comparison of the results revealed that the G-E composite showed the lowest tensile strength values. SiC-G-E composite showed the highest tensile strength value, confirming the reinforcing effect of SiC filler.

As recorded in Table II and also from Figure 5 elongation at break, decreased with the presence of filler. The reduction in percentage elongation at break of the composite was noticed in SiC-filled G-E composite as expected. SiC particles impose mechanical constraints in the mobility or deformability of

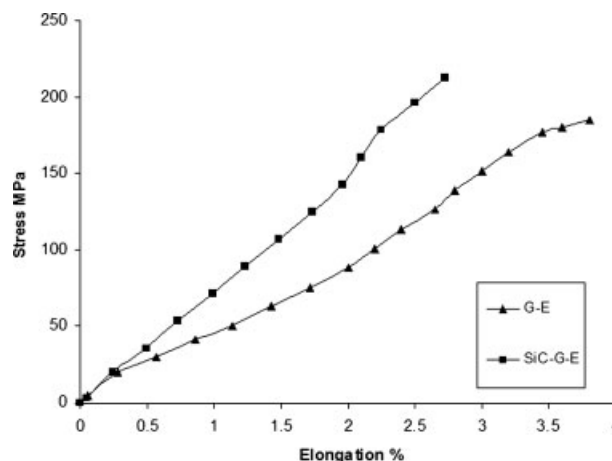


Figure 5 Stress-strain curves for G-E and SiC-G-E composites.

the matrix through the physical interaction between the filler and the matrix. The failure therefore propagates in a direction as dictated by the dispersoid concentration in the matrix. This means that the failure would propagate easily in those directions where the dispersoid concentration is less leading to increased tensile strength, tensile modulus, lower elongation, and increased surface hardness meaning better dimensional stability. The tests showed brittle fracture for the test samples.

The fibers in a polymer matrix composite are known to fail at different stress levels as the applied tensile load increases, and some main failure modes in tensile test are cited in literature.^{23,24} In this work, cracks at different cross sections of the specimen caused fiber-matrix debonding or shear failure of the matrix. These types of matrix shear failures and fiber-matrix debonding occurred either independently or in combination.

The load versus deflection curves for G-E and SiC-G-E composites are shown in Figure 6. The flexural strength data of the G-E and SiC-G-E composite are also recorded and given in Table II. From the results recorded, it is clear that the introduction of SiC filler in G-E composites increases the flexural strength. To explain this feature we used observations made during the duration of the test. It was observed that in

TABLE II
Mechanical Properties of G-P and SiC-G-P Composites

Property	G-E	SiC-G-E
Density, g/cc	1.802	1.844
Tensile strength, MPa	164.5	210.2
Tensile modulus, MPa	8559	14115
Tensile elongation at break (%)	3.8	2.7
Flexural strength, MPa	299.3	397.8
Flexural modulus, MPa	1230	2330
Surface hardness (HR _C)	102	120

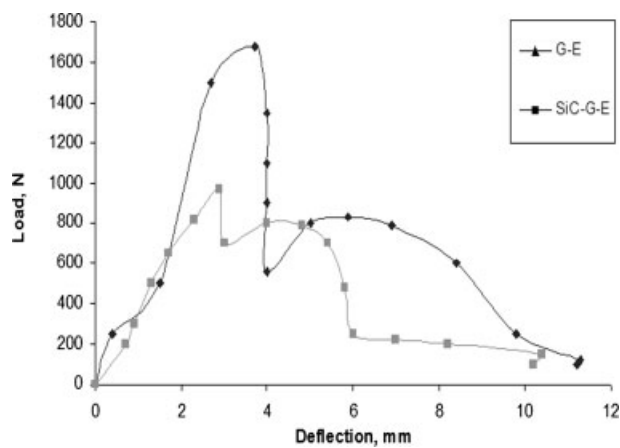


Figure 6 Load versus deflection curves for G-E and SiC-G-E composites.

almost all G-E samples, the failure process initiates first in the tensile side of the specimen and is followed by gradual and catastrophic failure. However, with SiC filled samples, the tensile region has noticeable fiber pullout features. This is in addition to ma-

trix cracking and fiber debonding noticed when compared to unfilled G-E samples. It should be pointed out that the presence of SiC fillers reduced voids in composite and that has been beneficial for the G-E composites.

The surface hardness of SiC-filled G-E composite is higher than that of unfilled G-E composite (Table II).

Fractographic analysis

The SEM micrographs in Figure 7(a,b) and Figure 8(a,b) showed the fractured surface of G-E and SiC-G-E composite systems, respectively. The fracture is due to delamination between the layers of the composite samples and fiber-pull out [Fig. 7(a)]. The SEM micrograph shown in Figure 7(b) indicates brittle fracture failure mechanism because as evident from the clean fibers on fractured surfaces. Other important failure mechanisms of composites such as fiber fracture (marked "b"), cohesive resin fracture (marked "c") and fiber-matrix debonding (marked "a") are also observed in SEM micrograph [Fig. 7(b)]. Generally matrix fracture was found to

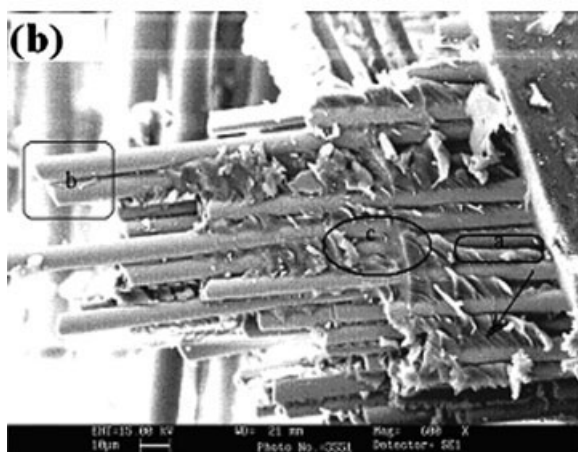
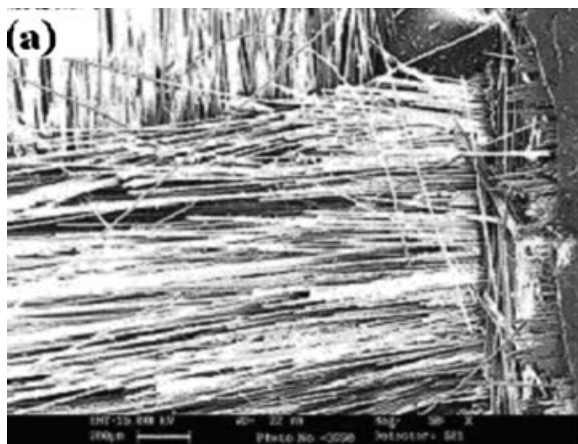


Figure 7 SEM picture of tensile fractured surface of G-E samples: (a) At $\times 50$ magnification; and (b) At $\times 600$ magnification.

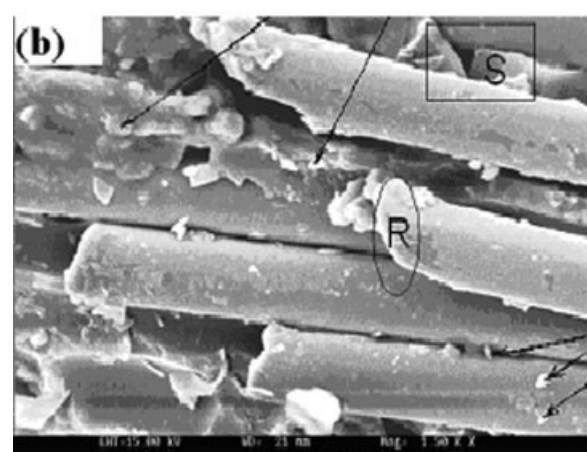
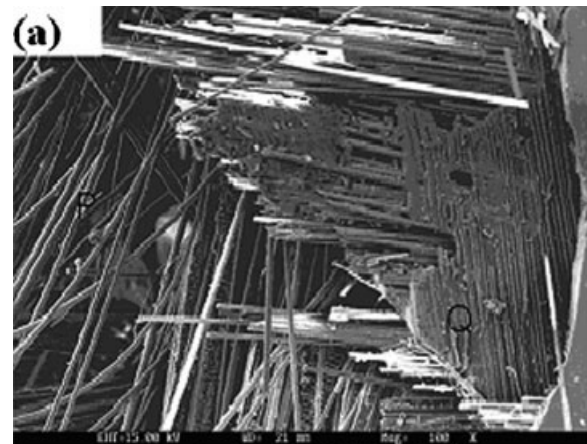


Figure 8 SEM picture of tensile fractured surface of SiC-G-E samples: (a) At $\times 100$ magnification; and (b) At $\times 1500$ magnification.

initiate at the surface of the fibers as indicated by the direction of river lines (marked by arrow) and propagates into the resin on either side, where cracks extend from the surfaces of adjacent fibers simultaneously.

SEM characterization of the SiC-G-E fractured surface shows [Fig. 8(a,b)] that the fibers are more or less covered with the matrix and SiC particles (marked by arrows). This is a qualitative indication of a greater interfacial strength between the fiber filler and the matrix. Disorientation of transverse fibers (marked "P"), fiber bridging (marked "Q"), fibers pull out, inclined fracture of longitudinal fibers (marked "R") and matrix cracking (marked "S") is also seen in SEM photomicrographs. The improvement reported in terms of mechanical properties of the composites evaluated is mainly due to the enhancement of adhesion or interfacial interactions among the fibers, matrix, and SiC filler.

CONCLUSIONS

The electrical properties such as dielectric loss and tan delta values are constant upto 10^3 MHz frequencies and abnormal behavior was noticed beyond 10^3 MHz frequencies. This may be because of phase and temperature changes, which causes abnormal variation in electrical properties of the composites beyond 10^3 MHz frequencies. After SiC loading a drastical change in dielectric constant of composite was noticed due to increase in conducting phase in the G-E composites.

Tensile, flexural, and hardness properties of unfilled and SiC-filled G-E composite systems have been evaluated. This work points to the fact that upon introduction of SiC filler in E-glass reinforced epoxy composite, there is an improvement in the mechanical properties, thus emphasizing the importance for the need to introduce fillers into glass reinforced epoxy composites.

SEM observations throw further light on features such as fiber bridging, matrix rollers, inclined fracture of fibers, disorientation of transverse fibers, and also showed good interfacial adhesion between epoxy matrix and glass fibers.

Correlating the tensile test results and SEM observations of the tensile fractured surface of the SiC-filled glass-epoxy composite, it is verified that the interfacial adhesion between fiber/matrix, leads to improved mechanical properties.

The authors are grateful to the Additional Director Dr. S. Seetharamu, Central Power Research Institute, Materials Testing Division, Bangalore for allowing them to use the laboratory facilities for this study. The authors are thankful to the Central Power Research Institute management for the permission extended to publish this article.

References

1. Vinson, J. R.; Chou, T. *Composite Materials and Their Uses in Structures*; Wiley: New York, 1975.
2. Sidney, H. G. *Handbook of Thermoset Plastic*, 2nd ed; William Andrew Inc.: New Jersey, 1998.
3. Matthews, F. L.; Rawlings, R. D. *Composite Materials: Engineering and Science*, 2nd ed.; Woodhead Publishing, CRC Press: Boca Raton, 1999.
4. Friedrich, K. Ed. *Friction and Wear of Polymer Composites Materials Series*; Elsevier: Amsterdam 1986; Vol. 1, p 233.
5. Kim, J.; Shioya, M.; Kobayashi, H.; Kaneko, J.; Kido, M. *Compos Sci Technol* 2004, 64, 2221.
6. Varada Rajulu, A.; Sanjeev Kumar, S. V.; Babu Rao, G.; Shashidhara, G. M.; Jiasong, H.; Jun, Z. *J Reinforced Plast Comp* 2002, 21, 1591.
7. Friedrich, K. *Compos Sci Technol* 1985, 22, 43.
8. Friedrich, K. In *Application of Fracture Mechanics of Composite Materials*; Friedrich, K., Ed., Amsterdam, New York, Netherlands, 1989; Chapter 11, p 425.
9. Karger-Kocsis, J. In *Application of Fracture Mechanics of Composite Materials*; Friedrich, K., Ed., Amsterdam, New York, Netherlands, 1989, Chapter 6, p 189.
10. Wassim, A.; Goknur, B. *J Reinforced Plast Compos* 2004, 23, 881.
11. Nielsen, M. L. *Mechanical Properties of Polymers and Composites*; Marcel Dekker: New York, 1974.
12. Hassaa, R.; Yahya, A. H.; Yahya; Tahir, A. R. *J Reinforced Plast Compos* 2004, 23, 969.
13. Suryasarathi, B.; Mahanwar, P. A. *J Miner Mater Character Engg* 2004, 3, 23.
14. Hayes, S. V.; Adams, D. F. *J Test Eval* 1982, 10, 61.
15. Parso, S.; Baptiste, D.; Decorbet, F.; Fitoussi, J.; Joannic, R. *Compos Sci Tech* 2002, 62, 579.
16. Viswanth, B.; Verma A. P.; Rao, C. V. S. K. *Wear* 1991, 145, 315.
17. Mody, P. B.; Chou, T. W.; Friedrich, K. *J Mater Sci* 1988, 23, 4319.
18. Broutman, L. J. In *Modern Composite Materials*; Broutman-Krock, Ed., Addison-Wesley Pub. Co.: USA, 1967, Chapter 13.
19. Boonstra, B. B.; Dannenberg, E. M. *Ind Eng Chem* 1954, 46, 218.
20. Carley, R. E.; Read, C.; Stow, C. D. *Br J Appl Phys D* 1969, 2, 567.
21. Bahder, G.; Garcia, F. G. *IEEE Trans, PAS-90* 1971, 3, 917.
22. Amin, A.; Hassan, H. H. *J Polym Sci, Polym Chem Ed* 1974, 12, 2651.
23. Smit, B. W. In *Engineering Materials Handbook*; Metals Park, OH: ASM, 1997; Vol. 1, p 786.
24. Master, J. E. In *Engineering Materials Handbook*; Metals Park, OH: ASM, 1997; Vol. 1, p 781.